Human T-lymphotrophic virus type I nucleocapsid protein NCp15: structural study and stability of the N-terminal zinc-finger

Françoise BERTOLA*, Claude MANIGAND*, Philippe PICARD*[1], Maya BELGHAZI† and Gilles PRECIGOUX*

*Unité de Biophysique Structurale, UMR 5471 CNRS, Bât B8, avenue des Facultés, Université de Bordeaux I, 33405 Talence Cedex, France, and †Institut Européen de Chimie Biologie, FRE 2247 CNRS, ENSCPB, Talence, France

An 18-residue peptide, corresponding to the minimum sequence of the N-terminal zinc-finger domain in the nucleocapsid of human T-lymphotrophic virus type I, was synthesized by a solid-phase method and fully characterized. Its ability to complex metal ions (Co^{2+} and Zn^{2+}) was clearly established by UV–visible spectroscopy and MS. The stability of these complexes was investigated by an original method with HPLC chromatography. Our results show that, even in the presence of air, the Zn^{2+} complex is highly stable. In contrast, the Co^{2+} complex undergoes a relatively fast degradation due to an intramolecular oxidation leading to the formation of a disulphide bridge between two cysteine residues. The ^{1}H-NMR analysis indicates that Zn^{2+} binds to the Nδ atom of the histidine residue rather than to the Nε atom. Two-dimensional NMR techniques were used to determine the solution structure of the zinc-finger, illustrated by the existence of turns in the overall conformation.

Key words: circular dichroism, mass spectrometry, peptide synthesis, solution structure, ultraviolet–visible spectroscopy.

INTRODUCTION

Human T-lymphotrophic virus type I (HTLV-I), which belongs to the oncoretrovirus family, has been recognized as the aetiological agent of adult T-cell leukaemia [1]. The virus is also associated with a chronic neurodegenerative syndrome termed HTLV-I-associated myelopathy or tropical spastic paraparesis ('HAM/TSP') [2,3]. Retroviruses contain different functional proteins, some of which have been widely studied in the structural plane, particularly HIV-1 and MMLV (Moloney-murine-leukaemia virus) [4–6]. As far as HTLV-I is concerned, only the structural characterization of the capsid protein has been described recently in the literature [7]. Here we report structural information on the nucleocapsid protein (NC) of HTLV-1 (NCp15), another essential protein of HTLV-I.

All retroviruses encode a Gag precursor polyprotein, produced in the host cell during the late stages of the infectious cycle. The Gag polyprotein is cleaved by the viral protease into several smaller proteins, including the nucleocapsid protein. In the viral particle, NC is a key component of the capsid and is in close contact with the dimeric RNA genome. The NC domain of the Gag precursor is critical for the recognition and packaging of the viral genome [8] and is important in viral particle formation [9,10]. Thus NC seems to be an interesting target for the development of an anti-retroviral therapy.

This small and highly basic protein contains one copy (MMLV) or two copies (HIV-1) of a conserved CCHC motif (Cys-Xaa$_2$-Cys-Xaa$_4$-His-Xaa$_4$-Cys). For MMLV and HIV-1, NC binds tightly to one or two equivalents of Zn^{2+} respectively, in a tetrahedral co-ordination leading to a structural domain called the zinc-finger [11–13]. In the case of HIV-1 it has been shown that the two zinc-finger domains are structurally similar [14] but not functionally equivalent [15]. Furthermore, the sequence of the N-terminal zinc-finger domain is highly conserved in all retroviruses [16]. This domain has a higher affinity for Zn^{2+} ions than the C-terminal domain [13]. It interacts specifically with the HIV-1 SL3 recognition element of the ΨRNA packaging signal [17,18]. Thus the N-terminal zinc-finger has a crucial role in the specific recognition of viral RNA sequences, whereas the C-terminal zinc-finger is dispensable for this interaction.

For HTLV-I, the completely expressed NCp15, with two CCHC motifs, was shown to bind Zn^{2+} ions with a high affinity (Western blot method) [19]. The present paper focuses on the first CCHC motif (the N-terminal domain of NCp15), an 18-residue sequence. To study the structure–function relationships of the NCp15 N-terminal zinc-finger, we first present the solid-phase synthesis of this peptide together with an original stability study of the corresponding metal finger by spectroscopy (UV–visible), chromatography (reverse-phase HPLC) and MS. We then describe the solution structure of the zinc-finger as found with CD and NMR spectroscopies.

EXPERIMENTAL

Peptide synthesis

The peptide was obtained by solid-phase peptide synthesis on an Applied Biosystems 431A peptide synthesizer with the t-butoxycarbonyl (Boc)/benzyl standard strategy on a Boc-Gln-4-(oxymethyl)phenylacetamidomethyl resin (0.5 mmol). After removal of the side-chain protections, the final resin was cleaved by classical treatment with HF (90 min, 0 °C). Crude peptide was first extracted with aqueous acetic acid, then diluted with water, freeze-dried and stored under N_2 at 0 °C.

HPLC analysis

Analytical HPLC was performed on a C_{18} Vydac column (4.6 mm × 250 mm, 300 Å pore size (1Å = 0.1 nm), 5 μm particle size) with a Waters 600E system controller and a Waters 996 photodiode array detector. Elution was achieved with a linear gradient of 10–60 % (v/v) acetonitrile containing 0.08 % (v/v)

Abbreviations used: Boc, t-butoxycarbonyl; DQF, double-quantum-filtered; ESI, electrospray ionization; HOHAHA, homonuclear Hartman–Hahn spectroscopy; HTLV-I, human T-lymphotrophic virus type I; MALDI, matrix-assisted laser-desorption ionization; MMLV, Moloney-murine-leukaemia virus; NC, nucleocapsid protein; NCp15; NC of HTLV-1.

[1] To whom correspondence should be addressed (e-mail p.picard@ubs.u-bordeaux.fr).

trifluoroacetic acid over 30 min, at a flow rate of 1 ml/min with detection at 220 nm. An identical column, with the same elution conditions, was used for the stability studies. Semi-preparative HPLC was performed on a C_{18} Vydac column (10 mm × 250 mm, 300 Å pore size, 5 μm particle size) with a linear gradient of 10–40 % (v/v) acetonitrile over 30 min with a Waters 510 apparatus equipped with a Waters 481 Lambdamax detector. To avoid possible oxidation of the cysteine residues, the HPLC-purified peptide samples were immediately freeze-dried after their elution. Their identity and purity were confirmed by amino acid analysis on a Millipore-Waters Pico-Tag workstation and by MS.

MS analysis

In MALDI (matrix-assisted laser desorption ionization) mode, a Bruker model Reflex III apparatus equipped with a laser source at 337 nm and a time-of-flight analyser was employed. Calibration was done with reference peptides over a 1060–5735 Da mass range (bradykinin, substance P, ACTH 18–39 and bovine insulin). The 18-residue peptide (1 μM) was dissolved in 50 % (v/v) acetonitrile containing 0.1 % (v/v) trifluoroacetic acid and mixed 1:1 with a matrix of α-cyano-4-hydroxycinnamic acid in the same solvent. This mixture (0.5 μl) was put on the target, dried at room temperature and introduced into the spectrometer.

In ESI (electrospray ionization) mode, analyses were performed on a Micromass LCTof model instrument equipped with an electrospray source and a time-of-flight analyser. Calibration was performed with horse heart apomyoglobin. Samples were introduced directly via a syringe pump (Harvard) at a constant flow rate of 5 μl/min, with a 10–20 μM concentration. Standard conditions used a water/methanol (1:1, v/v) mixture containing 1 % (v/v) acetic acid. For observation of the Zn^{2+} complex, the solvent was 20 mM ammonium acetate, pH 6.5.

For LC/MS experiments, a C_{18} column (1 mm × 150 mm, 300 Å pore size, 5 μm particle size) was used with the same eluant as for analytical HPLC, except that the trifluoroacetic acid concentration was decreased to 0.05 % (v/v), the flow rate was 50 μl/min and a splitter was inserted before the mass spectrometer, allowing a 20 μl/min flow rate to reach the electrospray source.

UV measurements

UV–visible absorption spectra were recorded from 250 to 800 nm on a Safas 190 DES spectrometer with quartz cells of 0.5 cm path length (Hellma). Samples (0.2 mM) were analysed in 20 mM phosphate buffer, pH 7.4, in the presence of 1.2 equiv. of Co^{2+} or Zn^{2+} ions. The spectra were corrected for background and free peptide interferences.

CD spectroscopy

The peptide samples (40 μM) were dissolved in 20 mM phosphate buffer, pH 7.4, containing 1.2 equiv. of Zn^{2+} ions. CD spectra were recorded at room temperature on a Mark VI Jobin Yvon dichrograph, between 184 and 270 nm, with a cell of 1 mm path length (increment 0.5 nm, bandwidth 2 nm, integration time 2 s). For each sample three spectra were collected and averaged and the background interference was corrected. The spectrum deconvolution was calculated by the Johnson method [20].

NMR spectroscopy

NMR samples were prepared by dissolving the peptide at 5 mM in $H_2O/^2H_2O$ (19:1, v/v) containing 20 mM sodium phosphate and 2 mM NaN_3. The pH was adjusted to 6.8 and a slight excess of $ZnCl_2$ (1.2 equiv.) was added to form the complex. Chemical shifts are expressed in p.p.m. relative to sodium 2,2-dimethyl-2-silapentane-5-sulphonate ('DSS'). All experiments were performed at 303 K on a Bruker DPX 400 spectrometer, operating at 400 MHz for protons, with the carrier frequency set to the water resonance. Two-dimensional NMR spectra were obtained in the phase-sensitive mode by using the method of time-proportional phase increments ('TPPI') [21]. Suppression of the water peak was achieved by presaturation of the solvent resonance during the relaxation delay (and during the mixing time of the NOESY experiments) or by watergate pulse sequences [22]. The spectral width was approx. 12 p.p.m. in both dimensions; 2048 data points were collected for each of the 512 t_1 recorded values. Mixing times of 100 and 200 ms were used in the homonuclear Hartman–Hahn spectroscopy (HOHAHA) and NOESY experiments respectively.

Data were processed with the GIFA software [23]. All free induction decays were multiplied by a $\pi/3$ shifted sine-bell window, combined with a Lorentz–Gauss transformation in both dimensions. After zero-filling to a final spectrum of 2048 × 2048 points and double Fourier transformation, baseline corrections were performed with polynomial functions.

Structure calculations

Spectral data analysis and proton assignments were realized with the XEASY program [24]. Distance constraints were obtained from cross-peak intensities of NOESY experiments. Non-experimental additional constraints were used to ensure the tetrahedral co-ordination of the Zn^{2+} atom. Structure calculations were performed with the aid of the DYANA program [25], with the use of standard protocols. Graphic analysis and structure comparison were performed with the MOLMOL program [26] on a Silicon Graphics O2 R5000 computer.

RESULTS AND DISCUSSION

The minimum sequence of the first NCp15 zinc-finger domain [27] corresponds to the 18-residue fragment Q^{-2}PCFRCGKAGHWSRDCTQ^{+2} (single-letter amino acid codes). An internal numbering scheme is used here in which the first cysteine residue of the zinc-finger is designated Cys^1.

The 18-residue peptide was synthesized with the Boc chemistry in the solid phase. The N-terminus was acetylated to avoid

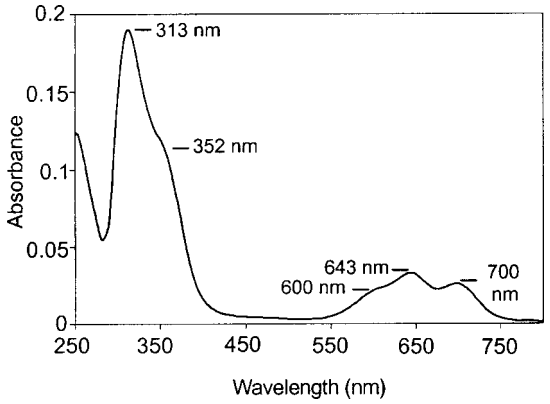

Figure 1 UV–visible absorption spectrum of the HTLV-I NC 18-residue peptide in a phosphate buffer, pH 7.4, in presence of 1.2 equiv. of $CoCl_2$

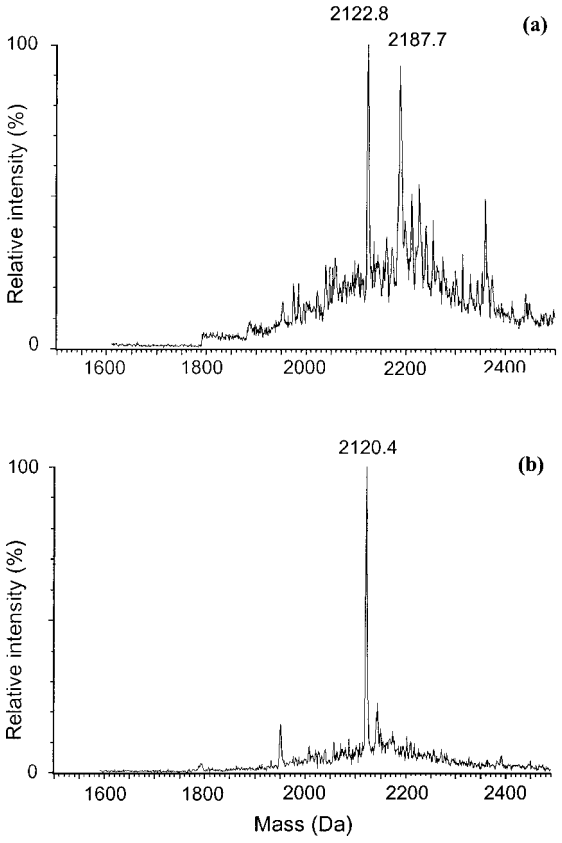

Figure 2 Mass spectra obtained in the electrospray ionization mode for the 18-residue peptide:

(**a**) Free and Zn complexed 18-residue peptide; (**b**) oxidized form P'_1 with an intramolecular disulphide bond.

parasitic electrostatic forces. A MALDI analysis (results not shown) confirmed the success of the synthesis: monoisotopic masses for the $(M+H)^+$ ions were $M_{exp} = 2121.77$ Da and $M_{calc} = 2121.92$ Da.

Characterization of peptide–metal complexes

The control of effective Zn^{2+} complexation by UV–visible absorption spectroscopy requires the previous co-ordination of an optically active ion such as Co^{2+} [12,28]. Metal co-ordination occurs via the nitrogen and sulphur atoms of histidine and cysteine residues respectively. In our case, the spectrum exhibits d–d electronic transition bands of the Co^{2+} ion at 643 and 700 nm, with a shoulder at 600 nm (Figure 1). This result is in accordance with the tetrahedral geometry described previously for the CCHC motif family [11,12]. Furthermore, in the UV region of the spectra, absorption bands at 313 and 352 nm appear, owing to a charge transfer from S^- to Co^{2+}, in accordance with published results on other peptides and proteins [29,30]. When performing spectroscopic studies at different pH values, we showed that metal co-ordination does not take place below pH 5.2, owing to histidine protonation.

The addition of $ZnCl_2$ to the Co^{2+} complex solution induces the disappearance of the characteristic d–d transition bands in the visible spectrum. This observation points to the ability of Zn^{2+} ions to replace Co^{2+} ions in the tetrahedral complex. These results confirm the effective formation of a zinc-finger with the synthetic 18-residue peptide of HTLV-I nucleocapsid protein. ESI–MS [31–33] was used to characterize this zinc-finger further, by infusing it in ammonium acetate buffer, pH 6.5. Under these conditions, a complex with a zinc atom was observed (average mass $M_{exp} = 2187.7 \pm 0.7$ Da; $M_{calc} = 2187.79$ Da) together with the apo-peptide (average mass $M_{exp} = 2122.8 \pm 0.6$ Da; $M_{calc} = 2122.40$ Da), as shown in Figure 2(a).

Stability studies

The stability of the peptide–metal complexes, implicating three sulphur atoms and one nitrogen atom, has been described previously in terms of dissociation constants determined by the titration of peptide solutions in the presence of Co^{2+} and Zn^{2+}. The Zn^{2+} co-ordination with these peptides was estimated to be 10^3–10^4-fold stronger than Co^{2+} co-ordination (with K_d^{Co} and K_d^{Zn} approx. 1 μM and 100 pM respectively) [11,29,30]. In the present study we performed a detailed investigation of the stability of the NC N-terminal cobalt-finger and zinc-finger by using UV–visible absorption spectroscopy and HPLC chromatography.

Kinetic studies of the cobalt-finger (prepared with 1 equiv. of Co^{2+}) showed that the complex is quite stable under anaerobic conditions. However, in the presence of air it undergoes a fast degradation ($K_d^{Co} = 50$ μM). During the degradation process, no evolution of the UV–visible absorption spectrum was observed (Figure 3a) when a fresh $CoCl_2$ solution was added to the peptide–Co^{2+} complex solution. In contrast, during the degradation of a peptide–Co^{2+} complex solution, prepared with a

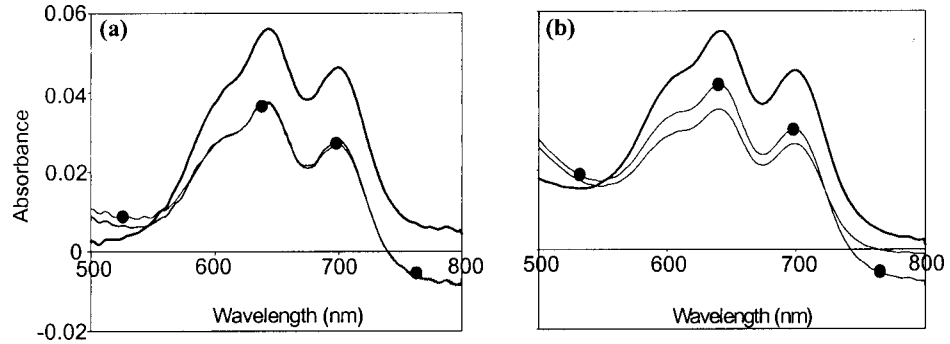

Figure 3 Evolution with time of the visible spectrum for the Co^{2+} complex

Freshly prepared solution (thick line); after 7 h (thin line); after 7 h followed by the addition (thin line with points) of Co^{2+} (**a**) or fresh peptide (**b**).

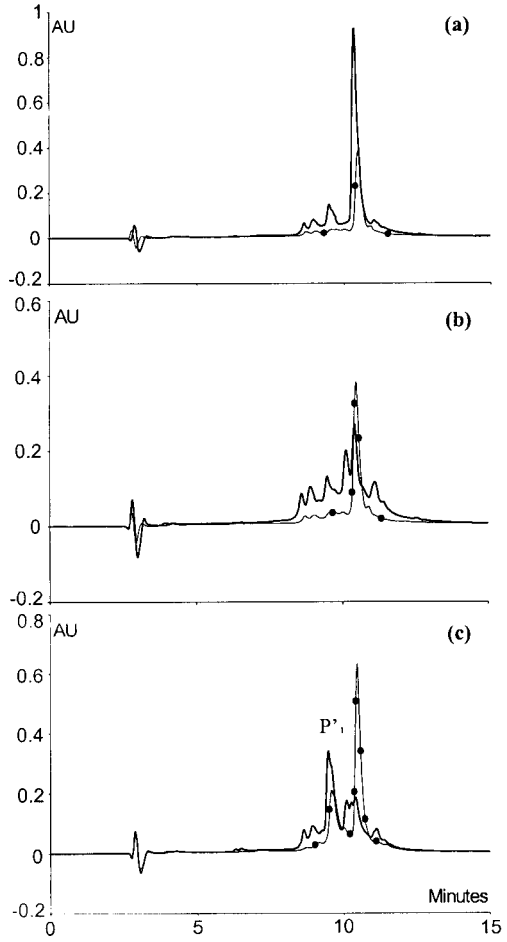

Figure 4 Time evolution of analytical HPLC chromatograms (220 nm)

(**a**) Co^{2+} (thick line) and Zn^{2+} (thin line with points) complex solution after 10 min; (**b**) the same as in (**a**) after 24 h; (**c**) free peptide solution after 10 min (thin line with points) and after 5 h (thick line).

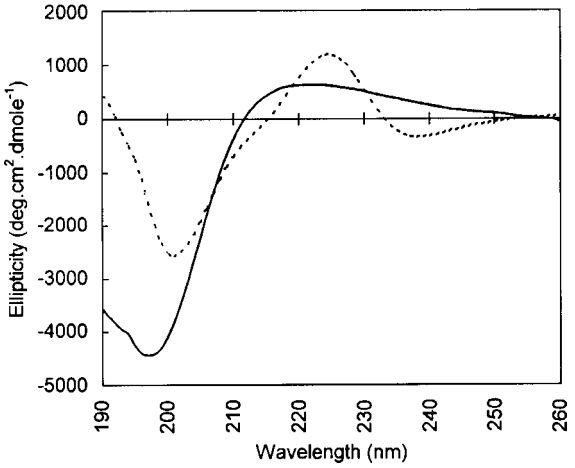

Figure 5 CD spectra of the HTLV-I NC 18-residue peptide in a phosphate buffer, pH 7.4, in the absence (thick line) and in the presence (dotted line) of 1.2 equiv. of $ZnCl_2$

slight deficit (0.9 equivalent) of Co^{2+}, the addition of a fresh peptide (P) solution induces a substantial increase in the characteristic bands of the complex (Figure 3b). These results suggest the oxidation of either the peptide–Co^{2+} complex holopeptide or the P apopeptide, leading to one or more oxidized peptide species unable to bind the metal, thus releasing Co^{2+} ions.

Another way of looking at the stability of the complex is to use HPLC chromatography, for which no relevant study has been described previously. For this purpose, different chromatographic analyses were performed. Because acidic elution conditions bring about decomplexation (histidine protonation), freshly prepared solutions of the metal complexes showed a major chromatographic signal with a retention time identical with that of the free peptide, for both the Co^{2+} and the Zn^{2+} complexes (Figure 4a). After 24 h the chromatographic profiles were completely different (Figure 4b). Oxidation of the Co^{2+} complex became obvious with the appearance of oxidized compounds (P′), whereas the Zn^{2+} complex remained quite stable. Chromatographic analysis of the free peptide in solution, under pH control, revealed its high instability. We observed the rapid formation of an oxidation P'_1 (Figure 4c). After 5 h the free peptide had almost disappeared, giving way to a mixture of 50 % P'_1 and 50 % secondary minor products, as over the course of time the structure of P'_1 changed. Using LC/MS, the P'_1 product has been identified as an intramolecular oxidation product corresponding to a disulphide bridge formation between two cysteine residues, i.e. there is a 2 Da mass difference between P and P'_1 peptides (average mass for the oxidized form $M_{exp} = 2120.4 \pm 0.2$ Da; $M_{calc} = 2120.38$ Da) (Figure 2b).

Thus, in contrast with UV–visible absorption spectroscopy, HPLC chromatography allows a direct and unambiguous control of Zn^{2+} ion co-ordination, examining the presence or absence of oxidation products. At the same time, total co-ordination is also indirectly proved by the absence of oxidation products.

Structural studies

The high stability of the first zinc-finger of NCp15 allowed us to undertake its structural study by CD and NMR spectroscopies. As a preliminary to NMR studies, CD spectroscopy is an efficient method for characterizing structures in solution and for studying conformational changes with solvent nature. It permits the investigation of the nature and the quantity of secondary structure elements in a peptide sequence. In our work, CD studies were performed on the 18-residue free peptide and the corresponding Zn^{2+} complex in phosphate buffer, pH 7.4 (Figure 5). The absence of both a positive maximum at 192 nm and negative bands at 222 and 208 nm, indicates that the structure of the 18-residue apo-peptide and holopeptide contains no α-helices. β-Sheets (negative and positive bands at 216 and 195 nm respectively) were not characterized. Thus both free peptide and Zn^{2+} complex proved not to be well structured in aqueous solution. Before the addition of Zn^{2+} ions, the CD spectrum was principally characteristic of a random-coil structure with a negative minimum at 198 nm and a broad positive band between 212 and 244 nm. After the addition of Zn^{2+} ions we noticed that the minimum was shifted from 198 to 201 nm and the positive peak was more pronounced at 225 nm. This evolution indicated the appearance of β-turn conformations [34,35], confirming the existence of a zinc-finger structure. A shoulder at 208 nm, specific for zinc-fingers [36], was also observed. Usually CD spectra are analysed empirically from a linear combination of standard spectra corresponding to well-defined structures such as α-helix and β-sheets, and to less well-defined structures such as β-turns and coils [37,38]. A singular value deconvolution method

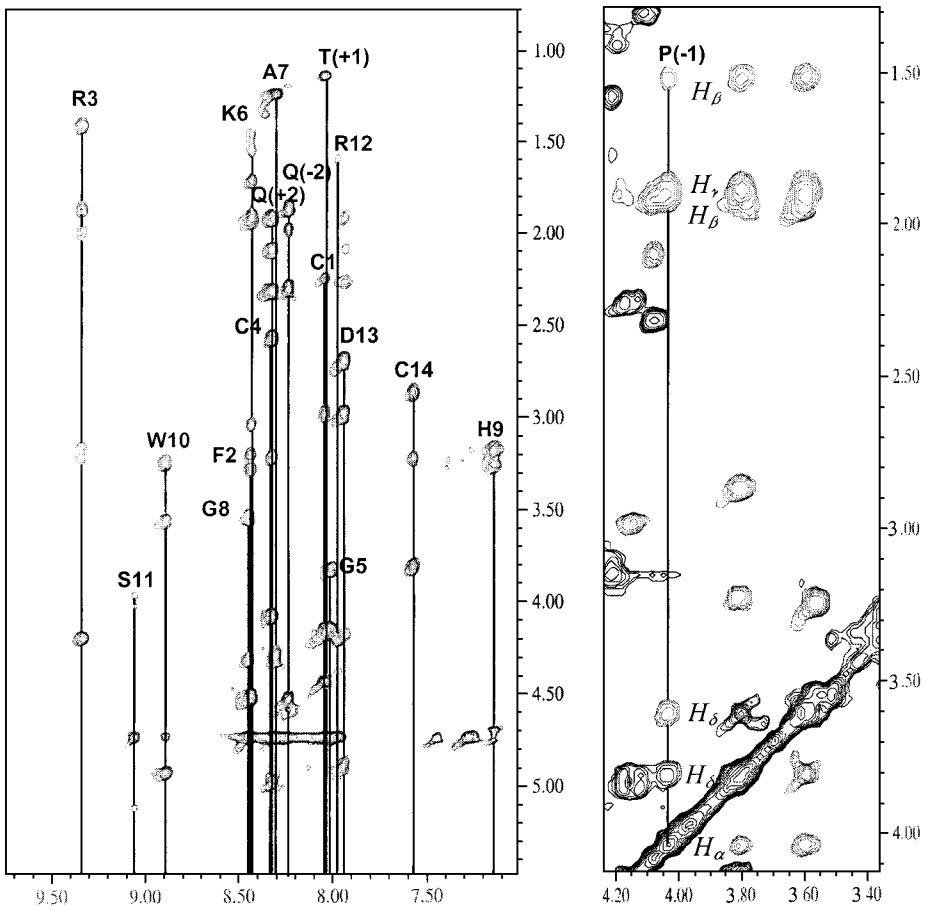

Figure 6 Portions of the HOHAHA spectrum of HTLV-I NC N-terminal zinc-finger acquired in H_2O, pH 6.8, at 300 K

All spin systems are indicated.

Table 1 ^{1}H NMR chemical shift assignments for the first zinc-finger of NCp15

Residue	Position	H_N	Hα	Hβ	Hγ	Hδ	Others
Gln	(−2)	8.24	4.53	1.98/1.87	2.30		ε 7/7.52
Pro	(−1)		4.04	1.93/1.52	1.88	3.80/3.60	
Cys	1	8.05	4.16	2.98/2.25			
Phe	2	8.44	4.50	3.27/3.19		7.32–7.38	ε and ξ 7.32–7.38
Arg	3	9.34	4.19	1.99/1.87	1.42	3.22/3.16	ε 7.29
Cys	4	8.33	4.97	3.21/2.57			
Gly	5	8.01	4.14/3.82				
Lys	6	8.44	4.52	1.92	1.55/1.46	1.72	ε 3.04
Ala	7	8.31	4.29	1.25			
Gly	8	8.45	4.30/3.53				
His	9	7.15	4.70	3.25/3.18		6.86	ε 7.44
Trp	10	8.90	4.92	3.56/3.25		7.39	ε 10.15 ξ 7.52/7.19 η 7.27
Ser	11	9.07	5.11	4.02/3.97			
Arg	12	7.98	4.20	1.77/1.67	1.58	3.14	ε 7.25
Asp	13	7.95	4.88	2.99/2.69			
Cys	14	7.59	3.81	3.22/2.87			
Thr	(+1)	8.05	4.44	4.44	1.14		
Gln	(+2)	8.32	4.07	2.09/1.92	2.32		ε 7/6.79

[20] is generally used to determine the respective quantities of these secondary structural elements. However, this method is reliable only for the well-characterized structures, i.e. α-helix or β-sheet contents. Percentages obtained for β-turns would present too many errors to have confidence in and they will be not discussed here.

NMR investigations are difficult for poorly defined structures. NMR specialist researchers usually therefore use a co-solvent

such as 1,1,1-trifluoroethanol, which promotes helix induction in aqueous solution for unstructured peptides with a propensity to form helices [39–41]. In our case, experimentally, no changes were observed when trifluoroethanol was added up to 50% (v/v), indicating the total absence of α-helix content from the molecule. In conclusion, whereas the 18-residue apopeptide (free peptide) of NCp15 was unstructured, the formation of the zinc-finger induced constraint turns. These results were confirmed by NMR studies.

For the ^{1}H NMR study, one-dimensional and two-dimensional experiments with HOHAHA [42], DQF (double-quantum-filtered) COSY [43] and NOESY [44,45] were performed on the Zn^{2+} complex. For the NOESY experiment, it should be noted that all the observed cross peaks were positive (negative nuclear Overhauser effects), indicating a rather long correlation time for a low-molecular-mass peptide and therefore a condition in which $\omega_0\tau_c > 1$ at the operating field of 400 MHz. Moreover, most of the NOESY cross peaks were present in a ROESY (rotating-frame Overhauser enhancement spectroscopy) spectrum performed on the same sample. However, we preferred to use the NOESY data because they permitted a more accurate determination of the interproton distances.

All of the spin systems were located with the aid of DQF-COSY and HOHAHA spectra (Figure 6). Their identification was achieved by using the uniqueness in the sequence (for Pro, Ala, Ser, Asp and His residues) and a sequential approach [46]. The complete list of assignments is presented in Table 1.

By an examination of the relative shielding of the histidine olefinic protons, there is strong evidence for a Zn^{2+} co-ordination to the Nδ nitrogen atom, as observed for the Rauscher murine leukaemia virus [47], rather than to the Nε as in the HIV-1 NC [48].

In the NOESY spectrum, the relatively intense NH(i)/NH($i+1$) correlations observed for the segments Arg^3-Cys-Gly^5 and Asp^{13}-Cys^{14} revealed the probable existence of turns in the structure. After the measurement of NOE cross-peak volumes, a first set of experimental distance restraints was obtained with the CALIBA module within the DYANA program. To include the Zn^{2+} ion in the peptide motif, two modified cysteine (CYZN) and histidine (HIZN) residues bearing a zinc pseudo-atom (van der Waals radius 0) and connected to the sulphur (bond length 2.3 Å) and δ nitrogen (bond length 2.0 Å) atoms, were added to the DYANA library. Then a Zn–Zn maximal distance of 0.05 Å was imposed to obtain the superposition of the four individual Zn pseudo-atoms and the creation of a single Zn site in the molecule [49]. Six non-experimental distance restraints were then introduced to ensure tetrahedral geometry around the metallic ion (3.8 Å for S–S and 3.6 Å for S–Nδ) [50]. From the local distance restraints and experimentally measured coupling constant values, the analysis of the local conformation around the Cα atom of each residue was performed with the HABAS module of the DYANA program; it resulted in a set of 60 dihedral angle restraints. Afterwards all the distance and angle restraints were used in the standard protocol of annealing with DYANA to generate 1000 structures. These structures were obtained from randomly generated conformations respecting the covalent structure parameters (bond lengths, bond angle, chiralities and planarities). They were then folded (torsion angle dynamics) to fit all the imposed restraints. The process was monitored with the value of a target function taking the role of a potential energy.

The 20 best structures, according to the smallest final target function value, were selected for further analysis. They presented no distance and dihedral angle violations exceeding 0.2 Å and 5° respectively. However, the relative scattering of these structures

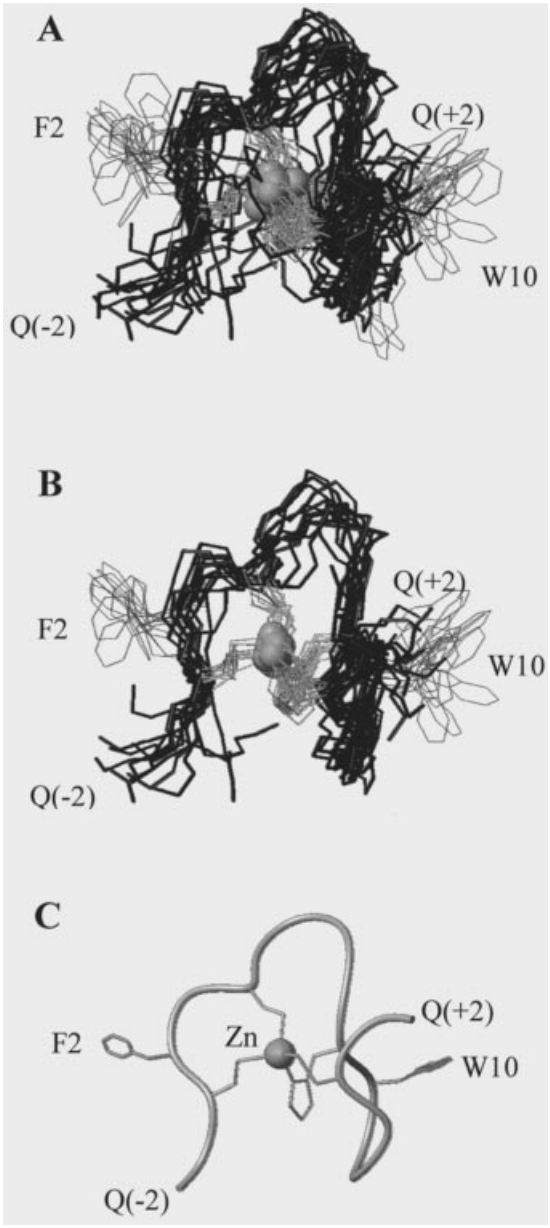

Figure 7 Structure of the HTLV-I NC N-terminal zinc-finger

(**A**) Superimposition on the backbone atoms of residues 1–14 for the 20 structures corresponding to the smallest final target function values; (**B**) same superimposition as in (**A**) for the 13 selected structures with a similar fold; (**C**) mean structure for this family. (**A**) and (**B**) show backbones (dark lines) plus selected side chains (fainter lines).

(Figure 7A) (average root-mean-square deviation 1.88 Å) is illustrative of the molecule's mobility and the weakness of unambiguous experimental restraints. The same paucity of NMR-derived structural restraints was observed for the N-terminal zinc-finger of the Mason–Pfizer monkey virus nucleocapsid [51].

Nevertheless, by superimposition of the backbone atoms of residues 1–14, we isolated, from the 20 best structures, a family of 13 structures (Figure 7B) with a quite similar folding (average root-mean-square deviation 1.13 Å). Their mean structure (Figure 7C) illustrates the existence of turns in the overall conformation, confirming the results obtained in CD studies.

The backbone fold is similar to that of the first HIV-1 NC zinc-finger [48,50]. Because of the folding, the hydrophobic side chains of Phe-2 and Trp-10 are directed towards the solvent. This orientation is in agreement with the participation, in specific RNA binding, of the equivalent residues Phe-2 and Thr-10 in the first zinc-finger of HIV-1 NC [17].

We thank P. Pellegrin and C. Aznar for their assistance with CD spectroscopy. This work was supported by a grant from the Comité départemental de la Dordogne de la Ligue Nationale Contre le Cancer.

REFERENCES

1 Poiesz, B. J., Ruscetti, F. W., Gazdar, A. F., Bunn, P. A., Minna, J. D. and Gallo, R. C. (1980) Detection and isolation of type C retrovirus particles from fresh and cultured lymphocytes of a patient with cutaneous T-cell lymphoma. Proc. Natl. Acad. Sci. U.S.A. **77**, 7415–7419

2 Gessain, A., Barin, F., Vernant, J. C., Gout, O., Maurs, L., Calender, A. and De Thé, G. (1985) Antibodies to human T-lymphotropic virus type-I in patients with tropical spastic paraparesis. Lancet **ii**, 407–410

3 Osame, M., Usuku, K., Izumo, S., Ijichi, N., Amitani, H., Igata, A., Matsumoto, M. and Tara, M. (1986) HTLV-I associated myelopathy, a new clinical entity. Lancet **i**, 1031–1032

4 Lodi, P. J., Ernst, J. A., Kuszewski, J., Hickman, A. B., Engelman, A., Craigie, R., Clore, G. M. and Gronenborn, A. M. (1995) Solution structure of the DNA binding domain of HIV-1 integrase. Biochemistry **34**, 9826–9833

5 Cai, M., Zheng, R., Caffrey, M., Craigie, R., Clore, G. M. and Gronenborn, A. M. (1997) Solution structure of the N-terminal zinc binding domain of HIV-1 integrase. Nat. Struct. Biol. **4**, 567–577

6 Clish, C. B., Peyton, D. H. and Barklis, E. (1998) Solution structures of human immunodeficiency virus type 1 (HIV-1) and moloney murine leukemia virus (MoMLV) capsid protein major-homology-region peptide analogs by NMR spectroscopy. Eur. J. Biochem. **257**, 69–77

7 Khorasanizadeh, S., Campos-Olivas, R. and Summers, M. F. (1999) Solution structure of the capsid protein from the human T-cell leukemia virus type-I. J. Mol. Biol. **291**, 491–505

8 Berkowitz, R. D., Ohagen, A., Hoglund, S. and Goff, S. P. (1995) Retroviral nucleocapsid domains mediate the specific recognition of genomic viral RNAs by chimeric Gag polyproteins during RNA packaging in vivo. J. Virol. **69**, 6445–6456

9 Darlix, J. -L., Lapadat-Tapolsky, M., De Rocquigny, H. and Roques, B. P. (1995) First glimpses at structure-function relationships of the nucleocapsid protein of retroviruses. J. Mol. Biol. **254**, 523–537

10 Dawson, L. and Yu, X. F. (1998) The role of nucleocapsid of HIV-1 in virus assembly. Virology **251**, 141–157

11 Roberts, W. J., Pan, T., Elliott, J. I., Coleman, J. E. and Williams, K. R. (1989) p10 single-stranded nucleic acid binding protein from murine leukemia virus binds metal ions via the peptide sequence Cys^{26}-X_2-Cys^{29}-X_4-His^{34}-X_4-Cys^{39}. Biochemistry **28**, 10043–10047

12 Fitzgerald, D. W. and Coleman, J. E. (1991) Physicochemical properties of cloned nucleocapsid protein from HIV. Interactions with metal ions. Biochemistry **30**, 5195–5201

13 Surovoy, A., Waidelich, D. and Jung, G. (1992) Nucleocapsid protein of HIV-1 and its Zn^{2+} complex formation analysis with electrospray mass spectrometry. FEBS Lett. **311**, 259–262

14 South, T. L., Blake, P. R., Hare, D. R. and Summers, M. F. (1991) C-terminal retroviral-type zinc finger domain from the HIV-1 nucleocapsid protein is structurally similar to the N-terminal zinc finger domain. Biochemistry **30**, 6342–6349

15 Gorelick, R. J., Chabot, D. J., Rein, A., Henderson, L. E. and Arthur, L. O. (1993) The two zinc fingers in the human immunodeficiency virus type 1 nucleocapsid protein are not functionally equivalent. J. Virol. **67**, 4027–4036

16 Summers, M. F. (1991) Zinc finger motif for single-stranded nucleic acids? Investigations by nuclear magnetic resonance. J. Cell. Biochem. **45**, 41–48

17 Dannull, J., Surovoy, A., Jung, G. and Moelling, K. (1994) Specific binding of HIV-1 nucleocapsid protein to PSI RNA *in vitro* requires N-terminal zinc finger and flanking basic amino acid residues. EMBO J. **13**, 1525–1533

18 De Guzman, R. N., Wu, Z. R., Stalling, C. C., Pappalardo, L., Borer, P. N. and Summers, M. F. (1998) Structure of the HIV-1 nucleocapsid protein bound to the SL3 psi-RNA recognition element. Science **279**, 384–388

19 Bess, J. W., Powell, P. J., Issaq, H. J., Schumack, L. J., Grimes, M. K., Henderson, L. E. and Arthur, L. O. (1992) Tightly bound zinc in human immunodeficiency virus type 1, human T-cell leukemia virus type I, and other retroviruses. J. Virol. **66**, 840–847

20 Johnson, Jr., W. C. (1990) Protein secondary structure and circular dichroism: a practical guide. Proteins: Struct., Funct., Genet. **7**, 205–214

21 Marion, D. and Wüthrich, K. (1983) Application of phase sensitive two-dimensional correlated spectroscopy (COSY) for measurements of ^1H-^1H spin-spin coupling constants in proteins. Biochem. Biophys. Res. Commun. **113**, 967–974

22 Piotto, M., Saudek, V. and Sklenar, V. (1992) Gradient-tailored excitation for single-quantum NMR spectroscopy of aqueous solutions. J. Biomol. NMR **2**, 661–665

23 Pons, J. L., Malliavin, T. E. and Delsuc, M. A. (1996) Gifa V4: a complete package for NMR data-set processing. J. Biomol. NMR **8**, 445–452

24 Bartels, C., Xia, T. H., Billeter, M., Güntert, P. and Wüthrich, K. (1995) The program XEASY for computed-supported NMR spectral analysis of biological macromolecules. J. Biomol. NMR **5**, 1–10

25 Güntert, P., Mumenthaler, C. and Wüthrich, K. (1997) Torsion angle dynamics for NMR structure calculation with the new program DYANA. J. Mol. Biol. **273**, 283–298

26 Koradi, R., Billeter, M. and Wüthrich, K. (1996) MOLMOL: a program for display and analysis of macromolecular structures. J. Mol. Graphics **14**, 29–32

27 Ratner, L., Philpott, T. and Trowbridge, D. B. (1991) Nucleotide sequence analysis of isolates of human T-lymphotropic virus type 1 of diverse geographical origins. AIDS Res. Hum. Retroviruses **7**, 923–941

28 Klemba, M. and Regan, L. (1995) Characterization of metal binding by a designed protein: single ligand substitutions at a tetrahedral Cys_2His_2 site. Biochemistry **34**, 10094–10100

29 Green, L. M. and Berg, J. M. (1990) Retroviral nucleocapsid protein-metal ion interactions: folding and sequence variants. Proc. Natl. Acad. Sci. U.S.A. **87**, 6403–6407

30 Griep, M. A., Adkins, B. J., Hromas, D., Johnson, S. and Miller, J. (1997) The tyrosine photophysics of a primase-derived peptide are sensitive to the peptide's zinc-bound state: proof that the bacterial primase hypothetical zinc finger sequence binds zinc. Biochemistry **36**, 544–553

31 Witkoska, H. E., Shackleton, C. H. L., Dahlman-Wright, K., Kim, J. Y. and Gustafsson, L. (1995) Mass spectrometric analysis of a native zinc-finger structure: the glucocorticoid receptor DNA binding domain. J. Am. Chem. Soc. **117**, 3319–3324

32 Loo, J. A., Holler, T. P., Foltin, S. K., McConnell, P., Banotai, C. A., Horne, N. M., Mueller, W. T., Stevenson, T. I. and Mack, D. P. (1998) Application of electrospray ionization mass spectrometry for studying human immunodeficiency virus protein complexes. Proteins. **2** (Suppl.), 28–37

33 Fukuda, H., Irie, K., Nakahara, A., Ohigashi, H. and Wender, P. A. (1999) Solid-phase synthesis, mass spectrometric analysis of the zinc-folding, and phorbol ester-binding studies of the 116-mer peptide containing the tandem cysteine-rich C1 domains of protein kinase C gamma. Bioorg. Med. Chem. **7**, 1213–1221

34 Brahms, S. and Brahms, J. (1980) Determination of protein secondary structure in solution by vacuum ultraviolet circular dichroism. J. Mol. Biol. **138**, 149–178

35 Laussac, J. -P., Cung, M. T., Erard, M. and Mazarguil, H. (1991) Etude par RMN et dichroïsme circulaire du peptide synthétique à 'doigt de zinc' de la protéine virale Gag de VIH-2. C. R. Acad. Sci. Paris, t. 313, série III, 183–186

36 Burke, C. J., Sanyal, G., Bruner, M. W., Ryan, J. A., LaFemina, R. L., Robbins, H. L., Zeft, A. S., Middaugh, C. R. and Cordingley, M. G. (1992) Structural implications of spectroscopic characterization of a putative zinc finger peptide from HIV-1 integrase. J. Biol. Chem. **267**, 9639–9644

37 Janin, J. and Delepierre, M. (1994) Biologie structurale-Principes et méthodes biophysiques, Hermann, Paris

38 Rodger, A. and Nordén, B. (1997) Circular dichroism and linear dichroism, Oxford University Press, New York

39 Dyson, H. J. and Wright, P. E. (1993) Peptide conformation and protein folding. Curr. Opin. Struct. Biol. **3**, 60–65

40 Jasanoff, A. and Fersht, A. R. (1994) Quantitative determination of helical propensities from trifluoroethanol titration curves. Biochemistry **33**, 2129–2135

41 Shiraki, K., Nishikawa, K. and Goto, Y. (1995) Trifluoroethanol-induced stabilization of the alpha-helical structure of beta-lactoglobulin: implication for non-hierarchical protein folding. J. Mol. Biol. **245**, 180–194

42 Bax, A. and Davies, D. G. (1985) MLEV-17-based two-dimensional homonuclear magnetization transfer spectroscopy. J. Magn. Reson. **65**, 355–360

43 Rance, M., Sorensen, O. W., Bodenhausen, G., Wagner, G., Ernst, R. R. and Wüthrich, K. (1983) Improved spectral resolution in cosy ^1H NMR spectra of proteins via double quantum filtering. Biochem. Biophys. Res. Commun. **117**, 479–485

44 Jeener, J., Meier, B. H., Bachmann, P. and Ernst, R. R. (1979) Investigation of exchange process by two-dimensional NMR spectroscopy. J. Chem. Phys. **71**, 4546–4553

45 Macura, S., Huang, Y., Suter, D. and Ernst, R. R. (1981) Two-dimensional chemical exchange and cross-relaxation spectroscopy of coupled nuclear spins. J. Magn. Reson. **43**, 259–281

46 Wüthrich, K. (1986) NMR of Proteins and Nucleic acids, Wiley, New York

47 Green, L. M. and Berg, J. M. (1989) A retroviral Cys-Xaa_2-Cys-Xaa_4-His-Xaa_4-Cys peptide binds metal ions: spectroscopic studies and a proposed three-dimensional structure. Proc. Natl. Acad. Sci. U.S.A. **86**, 4047–4051

48 Summers, M. F., South, T. L., Kim, B. and Hare, D. R. (1990) High-resolution structure of an HIV zinc fingerlike domain via a new NMR-based distance geometry approach. Biochemistry **29**, 329–340
49 Hoffman, R. C., Xu, R. X., Klevit, R. E. and Herriot, J. R. (1993) A simple method for the refinement of models derived from NMR data demonstrated on a zinc-finger domain from yeast ADR1. J. Magn. Reson. **B102**, 61–72
50 Morellet, N., Jullian, N., De Rocquigny, H., Maigret, B., Darlix, J.-L. and Roques, B. P. (1992) Determination of the structure of the nucleocapsid protein NCp7 from the human immunodeficiency virus type 1 by ^{1}H NMR. EMBO J. **11**, 3059–3065
51 Gao, Y., Kaluarachchi, K. and Giedroc, D. P. (1998) Solution structure and backbone dynamics of Mason-Pfizer monkey virus (MPMV) nucleocapsid protein. Protein Sci. **7**, 2265–2280

Received 22 June 2000/31 July 2000; accepted 15 September 2000